Published in final edited form as:
Cell Tissue Res. 2006 January ; 323(1): 53–70.

Postnatal developmental expression of the PDZ scaffolds Na^+-H^+ exchanger regulatory factors 1 and 2 in the rat cochlea

Refik Kanjhan*, **Deanne H. Hryciw**, **Mark C. Bellingham**, and **Philip Poronnik**
School of Biomedical Sciences, The University of Queensland, St Lucia, 4072, Queensland, Australia

C. Chris Yun
Division of Digestive Diseases, Emory University School of Medicine, Atlanta, GA 30322, USA

Abstract

Sensory transduction in the mammalian cochlea requires the maintenance of specialized fluid compartments with distinct ionic compositions. This is achieved by the concerted action of diverse ion channels and transporters, some of which can interact with the PDZ scaffolds, Na^+-H^+ exchanger regulatory factors 1 and 2 (NHERF-1, NHERF-2). Here, we report that NHERF-1 and NHERF-2 are widely expressed in the rat cochlea, and that their expression is developmentally regulated. Reverse transcription/polymerase chain reaction (RT-PCR) and Western blotting initially confirmed the RNA and protein expression of NHERFs. We then performed immunohistochemistry on cochlea during various stages of postnatal development. Prior to the onset of hearing (P8), NHERF-1 immunolabeling was prominently polarized to the apical membrane of cells lining the endolymphatic compartment, including the stereocilia and cuticular plates of the inner and outer hair cells, marginal cells of the stria vascularis, Reissner's epithelia, and tectorial membrane. With maturation (P21, P70), NHERF-1 immunolabeling was reduced in the above structures, whereas labeling increased in the apical membrane of the interdental cells of the spiral limbus and the inner and outer sulcus cells, Hensen's cells, the inner and outer pillar cells, Deiters cells, the inner border cells, spiral ligament fibrocytes, and spiral ganglion neurons (particularly type II). NHERF-1 expression in strial basal and intermediate cells was persistent. NHERF-2 immunolabeling was similar to that for NHERF-1 during postnatal development, with the exception of expression in the synaptic regions beneath the outer hair cells. NHERF-1 and NHERF-2 co-localized with glial fibrillary acidic protein and vimentin in glia. The cochlear localization of NHERF scaffolds suggests that they play important roles in the developmental regulation of ion transport, homeostasis, and auditory neurotransmission.

Keywords

EBP50; E3KARP; ERM-binding domain; Potassium channel; Purinergic signaling; Rat (Wistar, albino)

Introduction

The endolymph is a unique extracellular solution with an unusual ionic composition that is rich in K^+ (160 mM) and low in Na^+ (1.5 mM). This ionic composition is essential for the normal function of sensory hair cells in which K^+ provides the major charge carrier for sensory transduction process (Salt 2001; Wangemann 2002; Peters et al. 2004). In contrast, the

*e-mail: r.kanjhan@uq.edu.au, Tel.: +61-7-33651409, Fax: +61-7-33651766.

This project was supported by grants from the Australian Research Council, the National Health and Medical Research Council of Australia (P.P. and M.C.B.), and the National Institutes of Health (C.C.Y.).

perilymph is similar to other extracellular fluids with low K^+ and high Na^+. The epithelial cells lining the endolymphatic compartment form a polarized interface between these two fluid compartments and possess mechanisms for establishing these ion gradients. For example, active extrusion of Na^+ from the endolymph is necessary for cochlear sensory transduction process. Several pathways and mechanisms have been proposed to contribute to Na^+ reabsorption in the cochlea, including the amiloride-sensitive epithelial Na^+ channel in the apical membranes of strial marginal cells (Couloigner et al. 2001) and Reissner's membrane epithelium (Lee and Marcus 2003), the Na^+-H^+ exchanger isoform 3 (NHE3) in the apical membrane of strial marginal cells (Bond et al. 1998), and a Gd^{3+}-sensitive P2X2 purinoceptor-mediated non-selective cation current in outer sulcus cells (Lee et al. 2001). More recently, the Na^+-HCO_3^- co-transporter isoform 3 (NBC3) has been shown to be critical in dissipating the acid generated by neuronal and sensory cell activity (Bok et al. 2003).

In addition to the proteins directly involved in ion transport, there is increasing evidence that protein scaffolds play important roles in cochlear function (Verpy et al. 2000; Davies et al. 2001; Boeda et al. 2002; Mburu et al. 2003; Bao et al. 2004; Belyantseva et al. 2005; Kikkawa et al. 2005). For example, the postsynaptic density of the 95-kDa-disc large-zona occludens-1 (PDZ) domain protein harmonin has been shown to anchor cadherin 23 to the stereocilia microfilaments and is thought to contribute to shaping the hair bundle (Boeda et al. 2002). Mutations in harmonin have been implicated in Usher syndrome type 1C, which results in sensorineural deafness, vestibular dysfunction, and blindness (Verpy et al. 2000; Boeda et al. 2002). The interaction of another PDZ scaffold, whirlin, with myosin-XVa is also critical in normal hair-bundle morphogenesis (Mburu et al. 2003; Belyantseva et al. 2005; Kikkawa et al. 2005), and mutations in whirlin also result in deafness (Delprat et al. 2005).

Both NHE3 and NBC isoforms were originally described in kidney epithelial cells in which they were shown to interact with NHERF PDZ scaffolds. NHERF-1 (also called EBP50) was the first scaffold identified for an epithelial transporter and was found to mediate protein kinase A (PKA) inhibition of NHE3 in renal brush border vesicles (Weinman et al. 1995). Subsequently, its close relative NHERF-2 (also called E3KARP) was cloned and characterized (Yun et al. 1997). NHERF-1 and NHERF-2 consist of 358 and 337 amino acids, respectively, sharing 54% homology and possess two PDZ domains and a C-terminal ezrin-radixin-moesin-merlin (ERM)-binding domain that can interact with the actin cytoskeleton (Fanning and Anderson 1999; Shenolikar and Weinman 2001; Wade et al. 2003; Yun 2003; Shenolikar et al. 2004). NHERF-1 and NHERF-2 bind PDZ motifs in the C-termini of target proteins to assemble signaling/transport complexes at the plasma membrane. These target protein partners include channels and transporters, such as NHE3, NBC3, and the transient receptor potential channels (TRPC4 and TRPC5), the sodium-phosphate cotransporter (Na^+-Pi), and receptors, such as P2Y1 and β-adrenergic (Fanning and Anderson 1999; Shenolikar and Weinman 2001; Yun 2003; Shenolikar et al. 2004; Fam et al. 2005; Lee-Kwon et al. 2005; Weinman et al. 2005). NHERFs also serve to recruit signaling molecules, such as PKA, PKC, and PI-3 kinase, to the receptor complexes (Fanning and Anderson 1999; Shenolikar and Weinman 2001; Yun 2003; Shenolikar et al. 2004; Lee-Kwon et al. 2005; Weinman et al. 2005). Importantly, although NHERF-1 and NHERF-2 were originally described in the kidney, Northern blot analysis shows an overlapping and wide-spread distribution pattern for NHERF-1 and NHERF-2 mRNAs in human tissues, including brain, heart, colon, small intestine, liver, prostate, spleen, and placenta (Weinman et al. 1995; Yun et al. 1997). Immunohistochemical studies have demonstrated NHERF-1 and NHERF-2 in the human (Weinman et al. 2002) and mouse (Wade et al. 2003) kidney, NHERF-1 in the mouse retina (Nawrot et al. 2004) and Schwann cell processes (Gatto et al. 2003), and NHERF-2 in endothelia and pericytes from rat descending vasa recta (Lee-Kwon et al. 2005).

The finding that the cochlea possesses specialized epithelia that express NHE3 and NBC3 and the widespread distribution of NHERFs in the body raise the question as to whether NHERF-1 and NHERF-2 are present in the cochlea. The current study was therefore undertaken to investigate the expression and distribution of NHERF-1 and NHERF-2 in the rat cochlea during three stages of development at postnatal day (P) 8 (prior to onset of hearing), P21 (at maturation of hearing), and P70 (adult).

Materials and methods

All experiments were performed in accordance with the guidelines of the University of Queensland Animal Ethics Committee. Tissues for reverse transcription/polymerase chain reaction (RT-PCR), Western blotting, and immunohistochemistry were obtained from albino Wistar rats killed with sodium pentobarbitone (100 mg/kg; Valabarb, Jurox, Rutherford, NSW, Australia).

RT-PCR protocol

Total RNAwas extracted from snap-frozen P14–P26 albino Wistar rat cochleas (*n*=8) by using the Trizol reagent and following the manufacturer's instructions (Invitrogen, San Diego, CA). RNA (2 μg) was reverse-transcribed by using the One-step RT-PCR kit (Qiagen) with primers based on NHERF-1 and NHERF-2 mouse sequences. The primer sequences were as follows: NHERF-1 sense (5′-CTA AGC CAG GCC AGT TCA TCC GAG CAG T-3′) and antisense (5′-TGG GGT CAG AGG AGG AGG AGG AGG TAG A-3′), with a PCR product size of 447 bp (Ahn et al. 2001); NHERF-2 sense (5′-CTCAATGGTGGCTCTGCGTGC-3′) and antisense (5′-TGATTTCTGGGCASTGGCAGG-3′), with a PCR product size of 346 bp (Yun et al. 2002). The house-keeping gene, β-actin, was amplified as a control for the RT-PCR by using commercially available primers, giving a PCR product of 320 bp (Promega). Samples without reverse transcriptase were also run in parallel as a control. Thirty PCR cycles were run at 94° C, 55°C, and 72°C, for 1 min each. RT-PCR products were electrophoresed on a 2% agarose gel and visualized with ethidium bromide.

Western blotting

Cochleas were obtained from P21 albino Wistar rats (*n*=8). Tissues were homogenized in lysis buffer (50 mM TRIS-HCl pH 7.5, 150 mM NaCl, 1% Triton X-100, and Complete Protease inhibitors; Roche) by using a mortar. Samples were centrifuged at 12,000*g* for 10 min at 4°C. A 50-μg aliquot for each tissue was resolved by 7% SDS-polyacrylamide gel electrophoresis and then transferred to a nitrocellulose membrane (Bio-Rad). NHERF proteins were detected with polyclonal NHERF-1 (1:10,000) and NHERF-2 (1:1,000) antibodies. NHERF-1 polyclonal antibody was raised in rabbit against the recombinant protein from the carboxyl-terminal 105 amino acids of the NHERF-1 sequence (Yun et al. 2002). NHERF-2 polyclonal antibody (Ab2570) was raised in rabbit against the carboxyl-terminal 106 amino acids of NHERF-2 (Yun et al. 1998). In peptide competition, NHERF-1 and NHERF-2 antibodies (1:5,000) were incubated with a five-fold excess of their corresponding recombinant proteins at room temperature for 8 h and added to the nitrocellulose membranes overnight at 4°C. In reverse peptide competition experiments, antibodies were incubated with non-target peptides directed to other isoform (i.e., NHERF-1 antibody with NHERF-2 peptide and NHERF-2 antibody with NHERF-1 peptide) at five-fold excess, as for the peptide block experiments. A goat anti-rabbit secondary antibody conjugated to horseradish peroxidase (Pierce) at a dilution of 1:1,000 and SuperSignal Dura Extended Substrate (Pierce) were used to detect immunoblots as described previously (Hryciw et al. 2004).

Immunohistochemistry

Tissue preparation and immunocytochemical procedures were modified from previous studies (Housley et al. 1999; Kanjhan et al. 2004a). Five albino Wistar rats (10 cochleas; approximately 10 sections/cochlea) for each age group (P8, P21, and P70) were used for the analysis. After intracardiac perfusion with heparinized 0.9% NaCl solution containing 1.45 mM $NaNO_2$, the ears were fixed in situ with 4% formaldehyde freshly prepared from paraformaldehyde in 0.1 M phosphate buffer (pH 7.4). Ears were removed and post-fixed overnight at 4°C in the same fixative solution. Tissues were then cryoprotected in 10% and 30% sucrose in 0.1 M phosphate-buffered saline (PBS; pH 7.4). Sections (25–50 μm thick) were cut either in mid-modiolar or planar plane by using a cryostat and were subsequently permeabilised by using 0.5% Triton X-100 in 0.1 M PBS and blocked with 2% bovine serum albumin (BSA; Sigma, St Louis, Mo., USA) in PBS.

Free-floating cochlear sections were incubated for 8 h at 4°C in polyclonal rabbit NHERF-1 or NHERF-2 antibodies at 1:250 in PBS containing 2% BSA. Thereafter, sections were washed in PBS and then incubated for 6 h in secondary antibody (goat anti-rabbit IgG) conjugated to Texas Red sulfonyl chloride (TRSC; Jackson ImmunoResearch, West Grove, Pa., USA) at a 1:100 dilution. In double-labeling experiments, NHERF-1 or NHERF-2 immunolabeled sections were incubated for 11 h at 4°C with either mouse monoclonal glial fibrillary acidic protein (GFAP; 1:2,500; Sigma) or mouse polyclonal vimentin (1:250; Dakopatts, Sweden) antibodies in 0.1 M PBS containing 2% BSA. Sections were then washed in 0.1 M PBS prior to treatment in secondary anti-mouse IgG conjugated to fluorescein isothiocyanate (FITC; Silenus, Australia) at a 1:100 dilution (in 0.1 M PBS containing 2% BSA) for 6 h. The sections were washed with 0.1 M PBS prior to mounting. Control experiments, including incubations without the primary antibody (PBS control) and peptide block experiments in which the antibodies were pre-incubated (2 h) with their corresponding peptides at three-fold excess, were run in parallel.

After being immunolabeled, sections were mounted with a mounting medium containing 90% glycerol and 10% paraphenylenediamine (10 mg/ml in PBS; pH 8.0). Sections were viewed by using an Olympus BX60 microscope, and digital images were acquired with a cooled charge-coupled device camera, downloaded, and analyzed with Image-Pro Express software as previously described (Kanjhan et al. 2004a). Some of the immunolabeled cochlear sections (3–5 per group) were also examined by using a confocal microscope (Zeiss LSM 510 Meta) fitted with a Plan-Apochromat 100× oil objective. TRSC was excited at 534 nm, and emission was detected at 570 nm wavelength. Ten to 25 z-stacks (1 μm) per cochlear section were obtained at 1,024×1,024 size and 8 bit mode. Zeiss LSM Image Browser software (http://www.zeiss.com) was used for subsequent image analysis. Tissue preparation, immunohistochemical procedures, and image processing were performed in parallel and under identical conditions to allow comparisons between age groups. Tissue integrity (e.g., presence of stereocilia) was confirmed by light microscopy.

Results

Detection of NHERF-1 and NHERF-2 mRNA and protein in rat cochlea

NHERF-1 and NHERF-2 mRNA transcripts were detected in P14–P26 rat cochlea by using RT-PCR (Fig. 1a) as a single band at 447 bp corresponding to NHERF-1 and a band at 346 bp for NHERF-2 (Fig. 1a). In control experiments, in which the reverse transcriptase enzyme was omitted, no bands were detected (Fig. 1a), and β-actin was amplified as a single-band PCR product at 320 bp (Fig. 1a). NHERF-1 and NHERF-2 proteins were detected by Western blotting as single bands at approximately 52 kDa and 48 kDa, respectively, from P21 rat cochlea (Fig. 1b). Tissue samples from kidney and eye (known to express both proteins) were used as

controls (not shown). In order to confirm the specificity of the NHERF antibodies, the antibodies were pre-incubated with their corresponding peptides; this resulted in no bands appearing on the Western blot (Fig. 1b). The antibodies were also pre-incubated with the non-target peptides and the protein bands at the predicted sizes observed.

The specificity of NHERF antibodies for their targets was further supported by the immunohistochemical control experiments. Little background labeling was observed when the primary antibodies were omitted (Fig. 2j), and the NHERF-1 and NHERF-2 labeling was blocked when the antibodies were pre-incubated with their target peptides (Fig. 2k,l).

NHERF-1 labeling in the rat cochlea during postnatal development

Specific NHERF-1 and NHERF-2 immunolabeling in the rat cochlea was associated with significant changes between the postnatal developmental stages, particularly when compared between immature P8 (prior to onset of hearing) and mature P21 (immediately after onset of hearing; Table 1). NHERF-1 and NHERF-2 often showed an overlapping expression pattern within the same cochlear regions or cell groups, although several significant exceptions were also noted (Table 1).

Immunolabeling for NHERF-1 revealed a widespread distribution of NHERF-1 at all developmental stages examined (Table 1). In the immature P8 rat cochlea prior to the onset of hearing, intense NHERF-1 immunolabeling was mostly confined to the apical membrane of the cells lining the endolymphatic compartment (Figs. 2a–c, 3a, 4a,e, 5a,c, Table 1). Dense NHERF-1-labeled structures in the P8 cochlea included the stereocilia and cuticular plates of inner and outer hair cells (IHC and OHC; Figs. 3a, 4a), the apical membrane of strial marginal cells (Fig. 4e) and Reissner's epithelia (Figs. 3i, 5c), the apical surface of supporting cells in the organ of Corti including the inner and outer pillar cells, Hensen's cells, inner border cells (Figs. 3a, 4a), and the tectorial membrane particularly at the limbal zone near the insertion into the interdental cell area of the spiral limbus (Fig. 5a). In the immature organ of Corti, NHERF-1 labeling was particularly dense in the apical region between the IHC and the first row of OHC (Figs. 2c, 3a, 4a). Intense NHERF-1 labeling was also seen in the basal and intermediate cell region of the stria vascularis located between the strial marginal cells and the spiral ligament (Figs. 2a–c, 4e). Moderate NHERF-1 labeling was evident in a number of structures including the apical membrane of the spiral limbus interdental cells and fibrocytes (Figs. 2c, 5a), the inner and outer sulcus cells (Figs. 2c, 5a), spiral ligament fibrocytes (Figs. 2b,c, 4e), Claudius cells (Fig. 3a), spiral ganglion neurons (Figs. 2a,b, 3b, 4c), the walls of the large blood vessels including spiral modiolar artery and vein, and glial cells in the cochlear nerve (Fig. 2a).

In the P21 rat cochlea, upon completion of the onset of hearing, the distribution of NHERF-1 differed significantly from the P8 cochlea (Table 1, Figs. 2d–f, 3c,d, 4b,d,f, 5b,d,e). Most notably, the levels of NHERF-1 labeling were significantly reduced at the apical surfaces of the organ of Corti, including the hair cell stereocilia (compare Figs. 3c, 4b, 5e with Figs. 3a, 4a), the structural integrity of which was confirmed by light microscopy (Fig. 5f,h). The reduction in NHERF-1 labeling was also evident at the apical membranes of the marginal cells of the stria vascularis (compare Fig. 4e with Fig. 4f) and in the Reissner's membrane (compare Fig. 5c with Fig. 5d). This reduction was associated with an increase in NHERF-1 immunolabeling in other structures including the apical membranes of the interdental cells from the spiral limbus (compare Fig. 5a with Fig. 5b), the inner and outer sulcus cells (compare Fig. 5a with Fig. 5b), and the supporting cells of the organ of Corti including Hensen's, inner and outer pillar cells, inner border cells, and Deiters cells (compare Figs. 2f, 3c, 4b with Figs. 2c, 3a, 4a). In mature cochlea, dense labeling was detected by confocal analysis in Deiters cell processes extending in both basal and apical directions, the processes wrapping the outer hair cell bodies and reaching toward the cuticular plates (Fig. 4b). Increased NHERF-1 labeling was also observed in spiral ganglion neurons (compare Figs. 3d, 4d with Figs. 3b, 4c),

particularly in a subpopulation of small diameter neurons (arrows, Figs. 3d, 4d). The labeling in satellite cells associated with the spiral ganglion neurons remained weak between P8 and P21 (compare Fig. 4d with Fig. 4c). In the lateral wall, a small decrease of intensity in the basal and intermediate cell region of stria vascularis was observed (compare Figs. 2f, 4f with Figs. 2c, 4e). In other regions or cell groups, no significant change was observed in the intensity of NHERF-1 immunolabeling between P21 and P8 (Table 1), including glial cell bodies and processes located in the cochlear nerve (Fig. 8f).

In mature rat cochlea at P70, the NHERF-1 expression pattern was similar to that at P21; however, the differences between P70 and P8 were more pronounced than between P21 and P8 (Table 1, Figs. 2g–i, 3e–h). Small increases in NHERF-1 immunolabeling at P70 cochlea compared with P21 were seen in the inner sulcus cells (compare Fig. 2e with Fig. 2h) and spiral ganglion neurons (compare Figs. 2h, 3f with Figs. 2e, 3d). In contrast, a small decrease in NHERF-1 labeling at P70 cochlea compared with P21 was noted in the tectorial membrane and its limbal zone (compare Fig. 2d with Fig. 2g), Reissner's membrane (compare Fig. 2g–i with Fig. 2d,e), and hair cell soma and cuticular plate region (compare Fig. 3c with Fig. 3e). The walls of large blood vessels, including spiral modiolar artery and vein, located in the modiolus adjacent to the cochlear nerve showed strong expression at all layers including the endothelia, smooth muscle, and adventitia (Figs. 2g, 3g, 9d), with a similar labeling between age groups (compare Fig. 2a with Fig. 2g, see Table 1).

NHERF-2 in the rat cochlea during postnatal development

The expression pattern and developmental changes of NHERF-2 were mostly similar to those for NHERF-1 (Figs. 6, 7, 8, Table 1). In the immature P8 cochlea, intense NHERF-2 expression was located at apical membranes or structures of cells lining the endolymphatic compartment (Figs. 6a,b, 7a,e, 8a,c). These structures included IHC and OHC stereocilia and cuticular plates (Figs. 6a,b, 7a), apical terminals of supporting cells of the organ of Corti including the inner and outer pillar cells, Hensen's cells, and inner border cells (Figs. 6a, 7a), the apical membrane of marginal cells of the stria vascularis (Figs. 6a, 7e, 8c), the apical membrane of interdental cells of the spiral limbus (Figs. 6a, 8a), the apical surface of Reissner's membrane epithelia as a continuation of the labeling in the marginal cell layer (Figs. 6a, 8c), and the limbal zone of the tectorial membrane (Table 1). In the immature organ of Corti, NHERF-2 labeling was particularly dense in the apical region between the IHC and the first row of OHC (Figs. 6a,b, 7a). Moderate NHERF-2 immunolabeling was also evident in the basal and intermediate cell layers of the stria vascularis and fibrocytes of the spiral ligament (Figs. 6a, 7e), spiral ganglion neurons, and satellite cells (Fig. 7c) and of the walls of large blood vessels including spiral modiolar artery and vein and glial cells located in the cochlear nerve (Table 1). Interestingly, unlike NHERF-1, moderate NHERF-2 labeling was also seen at the synaptic region beneath the OHCs (Figs. 6b, 7b).

In the mature P21 cochlea, NHERF-2 immunolabeling was mostly reduced in the apical membranes lining the endolymphatic compartment (Figs. 5g, 6c,d, 7f, 8b,d, Table 1). NHERF-2 labeling in the hair cell stereocilia had diminished, whereas labeling of the cuticular plates of the hair cells was mostly maintained (compare Figs. 6d, 7b with Figs. 6b, 7a). The structural integrity of the stereocilia was confirmed by light microscopy (Fig. 5f,h). The intensity of the remaining NHERF-2 labeling of mature hair cell cuticular (apical) plates and the lack of labeling in stereocilia was also evident in planar cochlear sections (Fig. 6g–i). NHERF-2 labeling was reduced in the apical membranes of the strial marginal cells (compare Fig. 7e with Fig. 7f), limbal interdental cells (compare Fig. 8a with Fig. 8b), and the Reissner's epithelia (compare Fig. 8c with Fig. 8d). In contrast, NHERF-2 labeling was increased in the inner and outer sulcus cells (compare Figs. 6c, 8b with Figs. 6a, 8a), spiral ganglion neurons and satellite cells (compare Figs. 6c, 7d with Figs. 6a, 7c), synaptic regions beneath the OHCs

(compare Figs. 6d, 7b with Figs. 6b, 7a), supporting cells of the organ of Corti including Deiters and Hensen's cells and the inner and outer pillar and inner border cells (compare Figs. 6d, 7b with Figs. 6b, 7a), and the basal and intermediate cell region of the stria vascularis (compare Figs. 6c, 7f with Figs. 6a, 7e). NHERF-2 labeling intensity of the glial cell bodies and processes in the cochlear nerve did not show marked changes (Fig. 8e, Table 1).

NHERF-2 labeling was mostly associated with the plasma membranes and cellular process (e.g., stereocilia, axons, glial processes; Figs. 7, 8). However, unlike NHERF-1 labeling, punctate NHERF-2 labeling was also associated with the nucleus of several cell types including hair cells, supporting cells of the organ of Corti, spiral ganglion neurons, inner sulcus cells, and neuroglia (Figs. 7a–d, 8b,e). Nuclear labeling with NHERF-2 antibody was not seen in other cell types such as the strial marginal cell epithelia (Fig. 7e,f), Reissner's epithelia (Fig. 8c,d) and limbal interdental cells (Fig. 8a,b). NHERF-2 nuclear labeling in most of these cell types increased with maturation (compare Figs. 7b,d, 8b with Figs. 7a,c, 8a).

In the adult (P70) cochlea, NHERF-2 immunolabeling was mostly similar to P21 levels (Fig. 6e,f, Table 1). The densest NHERF-2 immunolabeling in the P70 organ of Corti was in the synaptic regions beneath the OHC (Fig. 6f) and in supporting cells of the organ of Corti, including the inner and outer pillar and Deiters cells (Fig. 6e,f). A marked increase in NHERF-2 immunolabeling was also evident in P70 compared with P8 and P21 in the subcentral and marginal regions of spiral ligament (compare Fig. 6a,c with Fig. 6e). A decrease in the intensity of NHERF-2 was also noted in the spiral limbus (compare Fig. 6c with Fig. 6e).

Co-localization of NHERF-1 and NHERF-2 with GFAP and vimentin

NHERF-1 and NHERF-2 localization in the cochlea was compared with the intermediate filament markers GFAP (a marker for several types of glial cells, including fibrous astrocytes and non-myelinating Schwann cells) and vim-entin (a marker for mesenchymal-derived cells, such as microglia and radial glia including retinal Müller and cerebellar Bergmann glia). NHERF-1 expression was seen in the cochlear nerve glial cells (e.g., astrocytes) identified by double-labeling with GFAP (Fig. 9a–c). NHERF-1 labeling in nerve covering (epineurium), external adventitia layer of large blood vessel walls, and glial cells (e.g., microglia) in the cochlear nerve was co-localized with vimentin (Fig. 9d–f). Various types of glial cells (e.g., astrocytes vs. microglia) were labeled with GFAP and vimentin antibodies respectively (compare Fig. 9e with Fig. 9h). NHERF-1 immunolabeling was co-localized with vimentin in Deiters cells in the adult organ of Corti (Fig. 9m–o) and in the strial basal and intermediate cells in which vimentin labeling was relatively weak (not shown). NHERF-2 immunolabeling in the cochlear nerve, epineurium, and walls of large blood vessels (including spiral modiolar artery and vein) was similar to that for NHERF-1 (compare Fig. 9d with Fig. 9g). NHERF-2 immunolabeling was co-localized with GFAP in a well-defined subpopulation of glial cells at the center of the nerve (Fig. 9g–i). NHERF-2 immunolabeling co-localized with vimentin in the nerve covering and the external adventitia layer of the large blood vessel walls (Fig. 9j–l). High-power confocal images showed NHERF-1 (Fig. 8f) and NHERF-2 (Fig. 8e) labeling in glial cells located in the cochlear nerve in which glial cell bodies and their processes were closely associated with capillaries and nerve coverings.

Discussion

This study reports the presence of NHERF-1 and NHERF-2 in the rat cochlea and changes in their expression during postnatal development. The major findings are (1) that both proteins exhibit an overlapping distribution pattern with a predominant apical localization in cells lining the endolymphatic compartment prior to the onset of hearing (P8), and (2) that significant changes occur on the maturation of hearing at P21, when the expression pattern of the NHERFs mainly shifts to other cell types including the supporting cells involved in ion transport,

recycling, and maintenance of cochlear homeostasis. These developmental changes in the expression pattern of NHERFs parallel the changes seen in the ionic composition of the endolymph, before and after the onset of hearing, i.e., the endolymph becomes rich in K^+ and low in Na^+ and Ca^{2+} with maturation (see Introduction; Salt 2001; Wangemann 2002; Peters et al. 2004).

The onset of hearing is associated with increased ionic and metabolic activity and with changes in cell proliferation and growth. It is clear from the literature that NHERFs play key roles in mediating a number of transport and signaling phenomena by forming macromolecular complexes of transporters, ion channels, receptors, and structural proteins (Hall et al. 1998; Fanning and Anderson 1999; Lederer et al. 2003; Pushkin et al. 2003; Yun 2003; Fam et al. 2005; Weinman et al. 2005). The rationale for the current study comes from the finding that the cochlea contains a number of proteins known to interact with NHERFs, plus numerous other proteins that have PDZ domains that could potentially interact with NHERFs. These cochlear proteins include NHE3 (Bond et al. 1998), the ERM family (Kitajiri et al. 2004), actin (Geal-Dor et al. 1993; Nishida et al. 1998), myosin (Boeda et al. 2002; Johnson et al. 2003; Mburu et al. 2003; Kitajiri et al. 2004; Belyantseva et al. 2005; Kikkawa et al. 2005), NBC3 (Bok et al. 2003), P2Y1 (Teixeira et al. 2000), β-adrenergic receptors (Fauser et al. 2004), the vacuolar proton pump v-H^+-ATPase (Stankovic et al. 1997), Na^+-K^+ ATPase (Ichimiya et al. 1994; Erichsen et al. 1996), growth factor receptors (Pickles and van Heumen 1997), glucocorticoid receptors (Erichsen et al. 1996), TASK-1 background K^+ channels (Kanjhan et al. 2004a), inwardly rectifying K^+ channels Kir1.1 (ROMK1) (Glowatzki et al. 1995), Kir4.1 and Kir5.1 (Hibino et al. 2004), aquaporin-4 (Mhatre et al. 2002), glutamate transporter GLAST (Furness and Lehre 1997), and plasma membrane Ca^{2+}-ATPase (Ichimiya et al. 1994; Dumont et al. 2001).

One of the most striking observed developmental changes was the down-regulation of NHERF-1 and NHERF-2 following maturation in the apical membrane of cells lining the endolymphatic compartment, including hair cell stereocilia, marginal cells of the stria vascularis, and Reissner's membrane epithelial cells. In contrast, expression of NHERFs was increased or maintained in the apical membranes of several other cell types facing the endolymphatic compartment, such as the inner and outer sulcus cells and the interdental cells of the spiral limbus, and of the supporting cells of the organ of Corti and the spiral ligament fibrocytes. These cell groups are known to be involved in the recycling of various ions including K^+, which is crucial for mechanotransduction process (Salt 2001; Wangemann 2002; Peters et al. 2004). Therefore, NHERFs may act as scaffolds to various ion channels (e.g., K^+ channels) and transporters along these pathways upon the maturation of hearing when K^+ recycling is required and metabolic activity is increased.

In the rodent cochlea, stereocilia sprout from the apical surface of sensory hair cells at embryonic day 15 and the hair bundles reach their final adult shape by P6, whereas the organ of Corti reaches its adult size by P10, becomes functional at around P12–P14, and is considered morphologically and functionally mature at P21 (Geal-Dor et al. 1993; Nishida et al. 1998). The temporal restriction of NHERF-1 and NHERF-2 expression in the immature hair cell stereocilia at P8 is consistent with developmental and transient expression in the hair cell stereocilia of other PDZ domain or binding proteins (e.g., ezrin, harmonin, and whirlin), which critically regulate development and morphogenesis (e.g., elongation) of cochlear stereocilia prior to the onset of hearing by binding target proteins such as myosin VIIa, cadherin 23, protocadherin 15, and Sans (Boeda et al. 2002; Johnson et al. 2003; Mburu et al. 2003; Kitajiri et al. 2004; Belyantseva et al. 2005; Kikkawa et al. 2005). The stereocilia are composed of bundles of actin filaments of which radixin is a prominent constituent (Kitajiri et al. 2004). After P14, ezrin expression in the stereocilia is replaced by radixin, the deficiency of which causes deafness by the degeneration of stereocilia (Kitajiri et al. 2004). Therefore, the

expression of ezrin correlates with NHERF-1 and NHERF-2 in the stereocilia during early postnatal development. Strong evidence has also been provided that NHERF-1 and NHERF-2 can organize ERM proteins in specific functional clusters at the plasma membrane (Morales et al. 2004). Therefore, NHERFs probably play a significant role in organizing actin and associated proteins in the developing stereocilia.

The marked decline in the expression of NHERFs in the apical membranes of strial marginal cells with the maturation of hearing was unexpected, given that these cells in the adult gerbil have been reported to express high levels of NHE3 solely in their apical membranes (Bond et al. 1998). The strong expression of NHERFs at the basal barrier, which is formed by basal and intermediate cells, suggests that these factors are involved with regulating ion transport and homeostasis at regions where the endocochlear potential is generated by KCNJ10 (Kir 4.1) channels located in the intermediate cells (Marcus et al. 2002; Gow et al. 2004; Wangemann et al. 2004; Spicer and Schulte 2005). NHERFs may spatially constrain Kir4.1 channels in intermediate cells. Spiral ligament fibrocytes express carbonic anhydrase and a Na-bicarbonate co-transporter (NBC3) essential for H^+/base transport, bicarbonate recycling, endolymph production, the maintenance of hair cell morphology, and normal auditory function (Salt 2001; Bok et al. 2003). NHERF-1 has been shown to be involved in interactions between the carboxy termini of NBC3 and the vacuolar proton pump v-H^+-ATPase (Pushkin et al. 2003).

The increased expression of NHERFs, particularly of NHERF-1, at the maturation of the supporting cells of the cochlea (e.g., Hensen's, inner and outer pillar, Deiters, and inner border cells), spiral ligament fibrocytes, inner sulcus, and spiral limbus suggests that they play a role in the cochlear K^+ cycling process (Salt 2001; Wangemann 2002; Peters et al. 2004). Increased expression of NHERFs in fibrocytes after the onset of hearing suggests their regulatory involvement in increased transporter and ionic activity. Extracellular ATP affects cochlear function by influencing the endocochlear potential, micromechanics, and neurotransmission via P2X and P2Ypurinergic receptors (Housley et al. 1999; Lee et al. 2001; Housley et al. 2002). The interaction of NHERF-2 with the PDZ-binding motif containing P2Y1 receptors (Hall et al. 1998; Fam et al. 2005) and the localization of P2Y1 receptors in sensory, supporting (e.g., Deiters cells and glia), and secretory cells of the cochlea (Teixeira et al. 2000), in which we have shown NHERF-2 expression, indicate a potential role for NHERFs in the modulation of purinergic signaling.

In spiral ganglion neurons, NHERF-1 immunolabeling intensity levels are notably increased at and after the onset of hearing, particularly in a small subpopulation of neurons that probably belong to the type II neurons comprising around 5% of the total population (Jagger and Housley 2003). Anatomical, functional, pharmacological, and biophysical properties of type II spiral ganglion neurons differ from those of type I that innervate IHCs (Jagger and Housley 2003). Type II neurons predominantly innervate OHCs, although recent studies have also shown a significant innervation, by their collaterals, of Deiters and Hensen's cells (Jagger and Housley 2003). However, NHERF-1 labeling is confined to the neuronal cell bodies (i.e., plasma membrane and cytoplasm). In contrast, NHERF-2 has been detected in the plasma membrane and nucleus and in the axons of spiral ganglion neurons. NHERF-2 labeling increases with maturation in both type I and type II spiral ganglion neurons and in their synaptic region beneath the OHC, suggesting involvement in the facilitation of synaptic efficiency between type II spiral ganglion neurons and OHC. On the other hand, a lack of detectable labeling for NHERFs in the IHC synaptic region suggests no direct role for NHERFs in the regulation of type-I-mediated synaptic transmission. The PSD-95 family of scaffolding proteins (e.g., PSD-93) have previously been localized at the synaptic region of OHCs (Davies et al. 2001). A recent study has demonstrated activity-dependent up-regulation of PSD-95 in spiral ganglion neurons by neuregulin-1 and Eos (Bao et al. 2004). NHERFs may also be regulated in spiral ganglion

neurons and at their synaptic regions with OHCs by similar neuroplastic and activity-dependent mechanisms.

The co-localization of NHERF-1 with vimentin in Deiters cells is consistent with the co-localization of NHERF-1 with cellular retinaldehyde-binding protein in mouse retinal Müller cells, which also express vimentin (Nawrot et al. 2004). NHERF-1 and NHERF-2 scaffolds co-localize with GFAP and vimentin in different types of glial cells in the cochlear nerve: GFAP-labeled astrocytes are located centrally and vimentin-labeled microglia are located in the nerve coverings. Accordingly, NHERF-1 has been reported to co-immunoprecipitate with TRPC4 in cultured astrocytes (Song et al. 2005), and the glutamate transporter GLAST expressed in glia has been shown to have a functional PDZ-binding motif (Marie and Attwell 1999). We have recently identified NHERF-1 protein co-immunoprecipitating with TASK-1 (unpublished observations), a developmentally regulated PDZ-domain-containing two-pore domain K^+ channel strongly expressed in radial and Bergmann glia in the central nervous system (Kanjhan et al. 2004b) and in the cochlea (Deiters and pillar cells and neuroglia; Kanjhan et al. 2004a). Cochlear glial cells, including spiral ganglion satellite cells, have previously been shown to express a number of Kir channels, e.g., Kir4.1 (Hibino et al. 2004). NHERF-1 and ERM proteins have also been reported in polarized Schwann cell processes where they have been implicated in the formation of the nodes of Ranvier (Gatto et al. 2003). NHERF-2 has recently been shown to co-localize with P2Y1 in glial cells, in which NHERF-2 interaction regulates P2Y1-mediated Ca^{2+} signaling (Fam et al. 2005). Thus, the presence of NHERF-1 and NHERF-2 in the glial cells located in the cochlear nerve and the spiral ganglion (satellite cells) is in keeping with its known expression in other glial cells. These results suggest important roles for NHERFs in supporting cells that closely interact with principal cells (e.g., neuroglial interaction) and that maintain a homeostatic environment for normal function.

In conclusion, we have found a broad and overlapping distribution of NHERF-1 and NHERF-2 in various cochlear cell types, including epithelia (sensory and supporting), neuron, glia (astrocyte and microglia), fibrocyte, endothelial, and smooth muscle cells. The localization of NHERFs in the cochlea is consistent with the expression of proteins known to interact with NHERF scaffolds in other tissues. The changes in expression during postnatal development strongly suggest diverse regulatory roles for NHERF-1 and NHERF-2 in the structural and functional development of the cochlea; they might interact with and facilitate the assembly of the macromolecular complexes involved in the growth, transport, and neurotransmission required for the development and maintenance of hearing.

Acknowledgements

We thank Prof. David J. Adams for support during the preparation of this manuscript.

References

Ahn W, Kim KH, Lee JA, Kim JY, Choi JY, Moe OW, Milgram SL, Muallem S, Lee MG. Regulatory interaction between the cystic fibrosis transmembrane conductance regulator and HCO_3^- salvage mechanisms in model systems and the mouse pancreatic duct. J Biol Chem 2001;276:17236–17243. [PubMed: 11278980]

Bao J, Lin H, Ouyang Y, Lei D, Osman A, Kim TW, Mei L, Dai P, Ohlemiller KK, Ambron RT. Activity-dependent transcription regulation of PSD-95 by neuregulin-1 and Eos. Nat Neurosci 2004;7:1250–1258. [PubMed: 15494726]

Belyantseva IA, Boger ET, Naz S, Frolenkov GI, Sellers JR, Ahmed ZM, Griffith AJ, Friedman TB. Myosin-XVa is required for tip localization of whirlin and differential elongation of hair-cell stereocilia. Nat Cell Biol 2005;7:148–156. [PubMed: 15654330]

Boeda B, El-Amraoui A, Bahloul A, Goodyear R, Daviet L, Blanchard S, Perfettini I, Fath KR, Shorte S, Reiners J, Houdusse A, Legrain P, Wolfrum U, Richardson G, Petit C. Myosin VIIa, harmonin and

cadherin 23, three Usher I gene products that cooperate to shape the sensory hair cell bundle. EMBO J 2002;21:6689–6699. [PubMed: 12485990]

Bok D, Galbraith G, Lopez I, Woodruff M, Nusinowitz S, BeltrandelRio H, Huang W, Zhao S, Geske R, Montgomery C, Van Sligtenhorst I, Friddle C, Platt K, Sparks MJ, Pushkin A, Abuladze N, Ishiyama A, Dukkipati R, Liu W, Kurtz I. Blindness and auditory impairment caused by loss of the sodium bicarbonate cotransporter NBC3. Nat Genet 2003;34:313–319. [PubMed: 12808454]

Bond BR, Ng LL, Schulte BA. Identification of mRNA transcripts and immunohistochemical localization of Na/H exchanger isoforms in gerbil inner ear. Hear Res 1998;123:1–9. [PubMed: 9745950]

Couloigner V, Fay M, Djelidi S, Farman N, Escoubet B, Runembert I, Sterkers O, Friedlander G, Ferrary E. Location and function of the epithelial Na channel in the cochlea. Am J Physiol Renal Fluid Electrolyte Physiol 2001;280:F214–F222. [PubMed: 11208596]

Davies C, Tingley D, Kachar B, Wenthold RJ, Petralia RS. Distribution of members of the PSD-95 family of MAGUK proteins at the synaptic region of inner and outer hair cells of the guinea pig cochlea. Synapse 2001;40:258–268. [PubMed: 11309841]

Delprat B, Michel V, Goodyear R, Yamasaki Y, Michalski N, El-Amraoui A, Perfettini I, Legrain P, Richardson G, Hardelin JP, Petit C. Myosin XVa and whirlin, two deafness gene products required for hair bundle growth, are located at the stereocilia tips and interact directly. Hum Mol Genet 2005;14:401–410. [PubMed: 15590698]

Dumont RA, Lins U, Filoteo AG, Penniston JT, Kachar B, Gillespie PG. Plasma membrane Ca^{2+}-ATPase isoform 2a is the PMCA of hair bundles. J Neurosci 2001;21:5066–5078. [PubMed: 11438582]

Erichsen S, Zuo J, Curtis L, Rarey K, Hultcrantz M. Na, K-ATPase α- and β-isoforms in the developing cochlea of the mouse. Hear Res 1996;100:143–149. [PubMed: 8922988]

Fam SR, Paquet M, Castleberry AM, Oller H, Lee CJ, Traynelis SF, Smith Y, Yun CC, Hall RA. $P2Y_1$ receptor signaling is controlled by interaction with the PDZ scaffold NHERF-2. Proc Natl Acad Sci U S A 2005;102:8042–8047. [PubMed: 15901899]

Fanning AS, Anderson JM. Protein modules as organizers of membrane structure. Curr Opin Cell Biol 1999;11:432–439. [PubMed: 10449334]

Fauser C, Schimanski S, Wangemann P. Localization of β1-adrenergic receptors in the cochlea and the vestibular labyrinth. J Membr Biol 2004;201:25–32. [PubMed: 15635809]

Furness DN, Lehre KP. Immunocytochemical localization of a high-affinity glutamate-aspartate transporter, GLAST, in the rat and guinea-pig cochlea. Eur J Neurosci 1997;9:1961–1969. [PubMed: 9383219]

Gatto CL, Walker BJ, Lambert S. Local ERM activation and dynamic growth cones at Schwann cell tips implicated in efficient formation of nodes of Ranvier. J Cell Biol 2003;162:489–498. [PubMed: 12900397]

Geal-Dor M, Freeman S, Li G, Sohmer H. Development of hearing in neonatal rats: air and bone conducted ABR thresholds. Hear Res 1993;69:236–242. [PubMed: 8226345]

Glowatzki E, Fakler G, Brandle U, Rexhausen U, Zenner HP, Ruppersberg JP, Fakler B. Subunit-dependent assembly of inward-rectifier K^+ channels. Proc R Soc Lond [Biol] 1995;261:251–261.

Gow A, Davies C, Southwood CM, Frolenkov G, Chrustowski M, Ng L, Yamauchi D, Marcus DC, Kachar B. Deafness in Claudin 11-null mice reveals the critical contribution of basal cell tight junctions to stria vascularis function. J Neurosci 2004;24:7051–7062. [PubMed: 15306639]

Hall RA, Ostedgaard LS, Premont RT, Blitzer JT, Rahman N, Welsh MJ, Lefkowitz RJ. A C-terminal motif found in the β2-adrenergic receptor, P2Y1 receptor and cystic fibrosis trans-membrane conductance regulator determines binding to the Na^+/H^+ exchanger regulatory factor family of PDZ proteins. Proc Natl Acad Sci U S A 1998;95:8496–8501. [PubMed: 9671706]

Hibino H, Higashi-Shingai K, Fujita A, Iwai K, Ishii M, Kurachi Y. Expression of an inwardly rectifying K^+ channel, Kir5.1, in specific types of fibrocytes in the cochlear lateral wall suggests its functional importance in the establishment of endocochlear potential. Eur J Neurosci 2004;19:76–84. [PubMed: 14750965]

Housley GD, Kanjhan R, Raybould NP, Greenwood D, Salih SG, Jarlebark L, Burton LD, Setz VC, Cannell MB, Soeller C, Christie DL, Usami S, Matsubara A, Yoshie H, Ryan AF, Thorne PR. Expression of the $P2X_2$ receptor subunit of the ATP-gated ion channel in the cochlea: implications

for sound transduction and auditory neurotransmission. J Neurosci 1999;19:8377–8388. [PubMed: 10493739]

Housley GD, Jagger DJ, Greenwood D, Raybould NP, Salih SG, Jarlebark LE, Vlajkovic SM, Kanjhan R, Nikolic P, Munoz DJ, Thorne PR. Purinergic regulation of sound transduction and auditory neurotransmission. Audiol Neuro-otol 2002;7:55–61.

Hryciw DH, Ekberg J, Lee A, Lensink IL, Kumar S, Guggino WB, Cook DI, Pollock CA, Poronnik P. Nedd4-2 functionally interacts with ClC-5: involvement in constitutive albumin endocytosis in proximal tubule cells. J Biol Chem 2004;279:54996–55007. [PubMed: 15489223]

Ichimiya I, Adams JC, Kimura RS. Immunolocalization of Na^+, K^+-ATPase, Ca^{2+}-ATPase, calcium-binding proteins, and carbonic anhydrase in the guinea pig inner ear. Acta Otolaryngol 1994;114:167–176. [PubMed: 8203199]

Jagger DJ, Housley GD. Membrane properties of type II spiral ganglion neurones identified in a neonatal rat cochlear slice. J Physiol (Lond) 2003;552:525–533. [PubMed: 14561834]

Johnson KR, Gagnon LH, Webb LS, Peters LL, Hawes NL, Chang B, Zheng QY. Mouse models of USH1C and DFNB18: phenotypic and molecular analyses of two new spontaneous mutations of the *Ush1c* gene. Hum Mol Genet 2003;12:3075–3086. [PubMed: 14519688]

Kanjhan R, Balke CL, Housley GD, Bellingham MC, Noakes PG. Developmental expression of two-pore domain K^+ channels, TASK-1 and TREK-1, in the rat cochlea. NeuroReport 2004a;15:437–441. [PubMed: 15094499]

Kanjhan R, Anselme AM, Noakes PG, Bellingham MC. Postnatal changes in TASK-1 and TREK-1 expression in rat brain stem and cerebellum. NeuroReport 2004b;15:1321–1324. [PubMed: 15167558]

Kikkawa Y, Mburu P, Morse S, Kominami R, Townsend S, Brown SD. Mutant analysis reveals whirlin as a dynamic organizer in the growing hair cell stereocilium. Hum Mol Genet 2005;14:391–400. [PubMed: 15590699]

Kitajiri S, Fukumoto K, Hata M, Sasaki H, Katsuno T, Nakagawa T, Ito J, Tsukita S. Radixin deficiency causes deafness associated with progressive degeneration of cochlear stereo-cilia. J Cell Biol 2004;166:559–570. [PubMed: 15314067]

Lederer ED, Khundmiri SJ, Weinman EJ. Role of NHERF-1 in regulation of the activity of Na-K ATPase and sodium-phosphate co-transport in epithelial cells. J Am Soc Nephrol 2003;14:1711–1719. [PubMed: 12819230]

Lee JH, Marcus DC. Endolymphatic sodium homeostasis by Reissner's membrane. Neuroscience 2003;119:3–8. [PubMed: 12763062]

Lee JH, Chiba T, Marcus DC. $P2X_2$ receptor mediates stimulation of parasensory cation absorption by cochlear outer sulcus cells and vestibular transitional cells. J Neurosci 2001;21:9168–9174. [PubMed: 11717350]

Lee-Kwon W, Wade JB, Zhang Z, Pallone TL, Weinman EJ. Expression of TRPC4 channel protein that interacts with NHERF-2 in rat descending vasa recta. Am J Physiol Cell Physiol 2005;288:C942–C949. [PubMed: 15590898]

Marcus DC, Wu T, Wangemann P, Kofuji P. KCNJ10 (Kir4.1) potassium channel knockout abolishes endocochlear potential. Am J Physiol Cell Physiol 2002;282:C403–C407. [PubMed: 11788352]

Marie H, Attwell D. C-terminal interactions modulate the affinity of GLAST glutamate transporters in salamander retinal glial cells. J Physiol (Lond) 1999;520 (Pt 2):393–397. [PubMed: 10523408]

Mburu P, Mustapha M, Varela A, Weil D, El-Amraoui A, Holme RH, Rump A, Hardisty RE, Blanchard S, Coimbra RS, Perfettini I, Parkinson N, Mallon AM, Glenister P, Rogers MJ, Paige AJ, Moir L, Clay J, Rosenthal A, Liu XZ, Blanco G, Steel KP, Petit C, Brown SD. Defects in whirlin, a PDZ domain molecule involved in stereocilia elongation, cause deafness in the whirler mouse and families with DFNB31. Nat Genet 2003;34:421–428. [PubMed: 12833159]

Mhatre AN, Stern RE, Li J, Lalwani AK. Aquaporin 4 expression in the mammalian inner ear and its role in hearing. Biochem Biophys Res Commun 2002;297:987–996. [PubMed: 12359252]

Morales FC, Takahashi Y, Kreimann EL, Georgescu MM. Ezrin-radixin-moesin (ERM)-binding phosphoprotein 50 organizes ERM proteins at the apical membrane of polarized epithelia. Proc Natl Acad Sci U S A 2004;101:17705–17710. [PubMed: 15591354]

Nawrot M, West K, Huang J, Possin DE, Bretscher A, Crabb JW, Saari JC. Cellular retinaldehyde-binding protein interacts with ERM-binding phosphoprotein 50 in retinal pigment epithelium. Invest Ophthalmol Vis Sci 2004;45:393–401. [PubMed: 14744877]

Nishida Y, Rivolta MN, Holley MC. Timed markers for the differentiation of the cuticular plate and stereocilia in hair cells from the mouse inner ear. J Comp Neurol 1998;395:18–28. [PubMed: 9590543]

Peters TA, Monnens LA, Cremers CW, Curfs JH. Genetic disorders of transporters/channels in the inner ear and their relation to the kidney. Pediatr Nephrol 2004;19:1194–1201. [PubMed: 15365806]

Pickles JO, van Heumen WR. The expression of messenger RNAs coding for growth factors, their receptors, and eph-class receptor tyrosine kinases in normal and ototoxically damaged chick cochleae. Dev Neurosci 1997;19:476–487. [PubMed: 9445085]

Pushkin A, Abuladze N, Newman D, Muronets V, Sassani P, Tatishchev S, Kurtz I. The COOH termini of NBC3 and the 56-kDa H^+-ATPase subunit are PDZ motifs involved in their interaction. Am J Physiol Cell Physiol 2003;284:C667–C673. [PubMed: 12444018]

Salt AN (2001) Dynamics of the inner ear fluids. In: Jahn AF, Santos-Saachi J (eds). Physiology of the ear. Singular, San Diego, pp 333–356

Shenolikar S, Weinman EJ. NHERF: targeting and trafficking membrane proteins. Am J Physiol Renal Fluid Electrolyte Physiol 2001;280:F389–F395. [PubMed: 11181400]

Shenolikar S, Voltz JW, Cunningham R, Weinman EJ. Regulation of ion transport by the NHERF family of PDZ proteins. Physiology (Bethesda) 2004;19:362–369. [PubMed: 15546854]

Song X, Zhao Y, Narcisse L, Duffy H, Kress Y, Lee S, Brosnan CF. Canonical transient receptor potential channel 4 (TRPC4) co-localizes with the scaffolding protein ZO-1 in human fetal astrocytes in culture. Glia 2005;49:418–429. [PubMed: 15540229]

Spicer SS, Schulte BA. Novel structures in marginal and intermediate cells presumably relate to functions of apical versus basal strial strata. Hear Res 2005;200:87–101. [PubMed: 15668041]

Stankovic KM, Brown D, Alper SL, Adams JC. Localization of pH regulating proteins H^+ATPase and Cl^-/HCO_3^- exchanger in the guinea pig inner ear. Hear Res 1997;114:21–34. [PubMed: 9447915]

Teixeira M, Butlen D, Ferrary E, Sterkers O, Escoubet B. Identification of uridine 5′-triphosphate receptor mRNA in rat cochlear tissues. Acta Otolaringol 2000;120:156–159.

Verpy E, Leibovici M, Zwaenepoel I, Liu XZ, Gal A, Salem N, Mansour A, Blanchard S, Kobayashi I, Keats BJ, Slim R, Petit C. A defect in harmonin, a PDZ domain-containing protein expressed in the inner ear sensory hair cells, underlies Usher syndrome type 1C. Nat Genet 2000;26:51–55. [PubMed: 10973247]

Wade JB, Liu J, Coleman RA, Cunningham R, Steplock DA, Lee-Kwon W, Pallone TL, Shenolikar S, Weinman EJ. Localization and interaction of NHERF isoforms in the renal proximal tubule of the mouse. Am J Physiol Cell Physiol 2003;285:C1494–C1503. [PubMed: 12917102]

Wangemann P. K^+ cycling and the endocochlear potential. Hear Res 2002;165:1–9. [PubMed: 12031509]

Wangemann P, Itza EM, Albrecht B, Wu T, Jabba SV, Maganti RJ, Lee JH, Everett LA, Wall SM, Royaux IE, Green ED, Marcus DC. Loss of KCNJ10 protein expression abolishes endocochlear potential and causes deafness in Pendred syndrome mouse model. BMC Med 2004;2:30. [PubMed: 15320950]

Weinman EJ, Steplock D, Wang Y, Shenolikar S. Characterization of a protein cofactor that mediates protein kinase A regulation of the renal brush border membrane Na^+-H^+ exchanger. J Clin Invest 1995;95:2143–2149. [PubMed: 7738182]

Weinman EJ, Lakkis J, Akom M, Wali RK, Drachenberg CB, Coleman RA, Wade JB. Expression of NHERF-1, NHERF-2, PDGFR-α, and PDGFR-β in normal human kidneys and in renal transplant rejection. Pathobiology 2002;70:314–323. [PubMed: 12865627]

Weinman EJ, Cunningham R, Shenolikar S. NHERF and regulation of the renal sodium-hydrogen exchanger NHE3. Pflugers Arch 2005;450:137–144. [PubMed: 15742180]

Yun CC. Concerted roles of SGK1 and the Na^+/H^+ exchanger regulatory factor 2 (NHERF2) in regulation of NHE3. Cell Physiol Biochem 2003;13:29–40. [PubMed: 12649600]

Yun CH, Oh S, Zizak M, Steplock D, Tsao S, Tse CM, Weinman EJ, Donowitz M. cAMP-mediated inhibition of the epithelial brush border Na^+/H^+ exchanger, NHE3, requires an associated regulatory protein. Proc Natl Acad Sci U S A 1997;94:3010–3015. [PubMed: 9096337]

Yun CH, Lamprecht G, Forster DV, Sidor A. NHE3 kinase A regulatory protein E3KARP binds the epithelial brush border Na^+/H^+ exchanger NHE3 and the cytoskeletal protein ezrin. J Biol Chem 1998;273:25856–25863. [PubMed: 9748260]

Yun CC, Chen Y, Lang F. Glucocorticoid activation of Na^+/H^+ exchanger isoform 3 revisited. The roles of SGK1 and NHERF2. J Biol Chem 2002;277:7676–7683. [PubMed: 11751930]

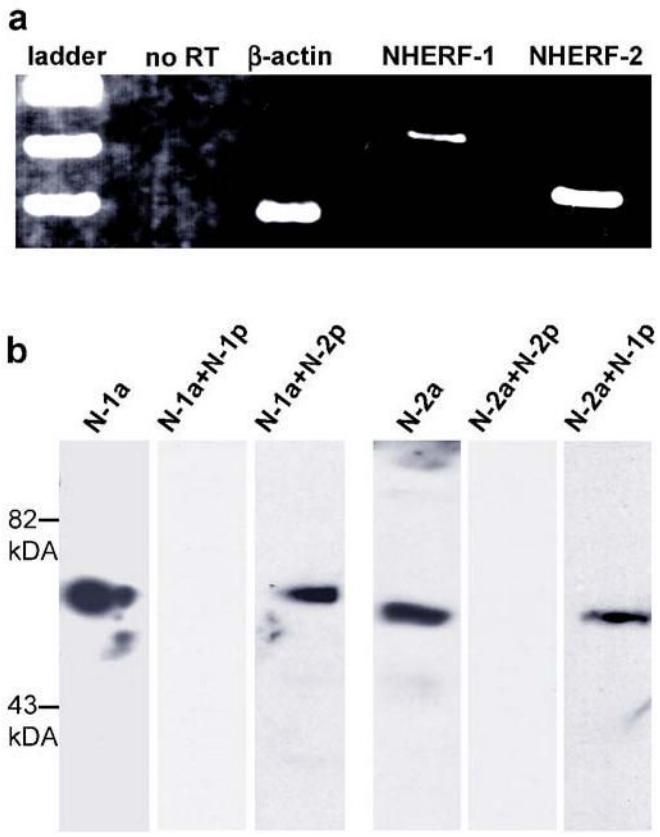

Fig. 1.

a Detection of NHERF-1 and NHERF-2 mRNA transcripts in the P14 rat cochlea by RT-PCR. NHERF-1 and NHERF-2 mRNA transcripts were detected as single bands at predicted 447 and 346 bp, respectively. A house-keeping gene, β-actin, was amplified as a control for the RT-PCR and was seen as a strong single band at 320 bp. No band was detected when the reverse transcriptase enzyme was omitted (*no RT*). The *ladder* indicates band sizes from 300 to 500 bp at 100-bp intervals. **b** Detection of NHERF-1 and NHERF-2 proteins as a single band at the predicted size of approximately 52 kDa and 48 kDa respectively in the P21 rat cochlea by Western blotting. The bands detected by NHERF-1 and NHERF-2 antibodies (*N-1a*, *N-2a*) were blocked when the antibodies were pre-incubated with their corresponding target peptides (*N-1a+N-1p*, *N-2a+ N-2p*). The bands were not blocked when the antibodies were pre-incubated with other peptides (*N-1a+N-2p*, *N-2a+N-1p*). Each lane was loaded with 50 μg tissue lysate

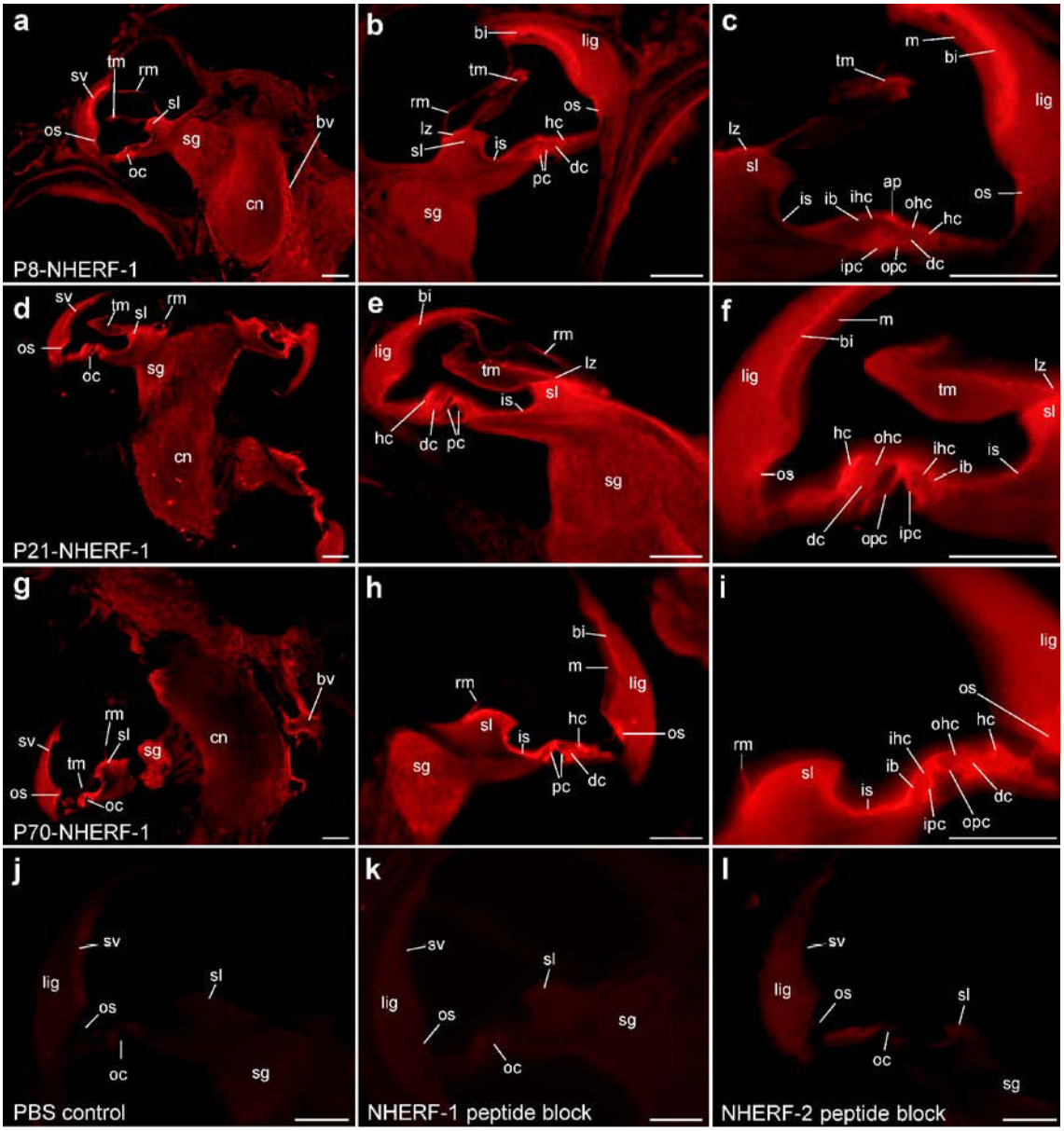

Fig. 2.

NHERF-1 immunolabeling in newborn (*P8*), juvenile (*P21*), and adult (*P70*) rat cochlea in cross section (*a* artery, *ad* tunica adventitia or the outermost layer of the blood vessel wall, *ap* apical membrane, *ax* axon, *bi* basal and intermediate cell region of the stria vascularis, *bl* basolateral membrane, *bv* blood vessel, *ca* capillary, *cc* Claudius cells, *cn* cochlear nerve, *dc* Deiters cells, *ep* epithelial cells of the Reissner's membrane, *et* endothelium layer of the blood vessel wall, *fi* fibrocytes, *g* glial cell, *hc* Hensen's cells, *ib* inner border cell, *ic* interdental cells, *ihc* inner hair cell, *ipc* inner pillar cell, *is* inner sulcus, *lig* spiral ligament, *lz* limbal zone of the tectorial membrane, *m* marginal cells of the stria vascularis, *mr* marginal region of the spiral ligament, *n* nucleus, *nc* nerve covering or epineurium, *oc* organ of Corti, *ohc* outer hair cell, *opc* outer pillar cell, *os* outer sulcus, *pc* pillar cells, *rm* Reissner's membrane, *s* satellite cell, *sc* subcentral region of the spiral ligament, *sg* spiral ganglion, *sl* spiral limbus, *sml* smooth muscle layer of the blood vessel wall, *sr* synaptic region, *stc* stereocilia and cuticular plates, *sv* stria vascularis, *tm* tectorial membrane, *v* vein); conventional fluorescence microscopy. **a**–

c NHERF-1 labeling in the P8 rat cochlea. The densest labeling was seen in the basal and intermediate cells of the stria vascularis. Dense labeling was seen in the stereocilia of the inner and outer hair cells, the apical end (i.e., cuticular plates) of the inner and outer pillar cells facing the endolymph, and the limbal zone of the tectorial membrane. **d–f** NHERF-1 labeling in the P21 rat cochlea. The densest labeling was located to Hensen's cells. Dense labeling was seen at the spiral limbus, Deiters cells, inner and outer pillar cells, and limbal zone of the tectorial membrane. **g–i** NHERF-1 labeling in the P70 rat cochlea. The most intense labeling was seen in Hensen's cells and the inner and outer pillar cells. Labeling was dense in the inner sulcus cells, interdental cells, and a subpopulation of spiral ganglion neurons. **j** PBS control; primary antibodies were omitted. Low level of background labeling in P70 cochlea. **k–l** Blocking of immunolabeling in P21 cochlea when NHERF-1 and NHERF-2 antibodies were incubated with their corresponding peptides. Note that, in albino rats, the intermediate cells occupy significantly less volume than in normal rats, with a compensatory increase in the marginal cell layer (see also Fig. 6a,c,e). *Bar* 100 μm

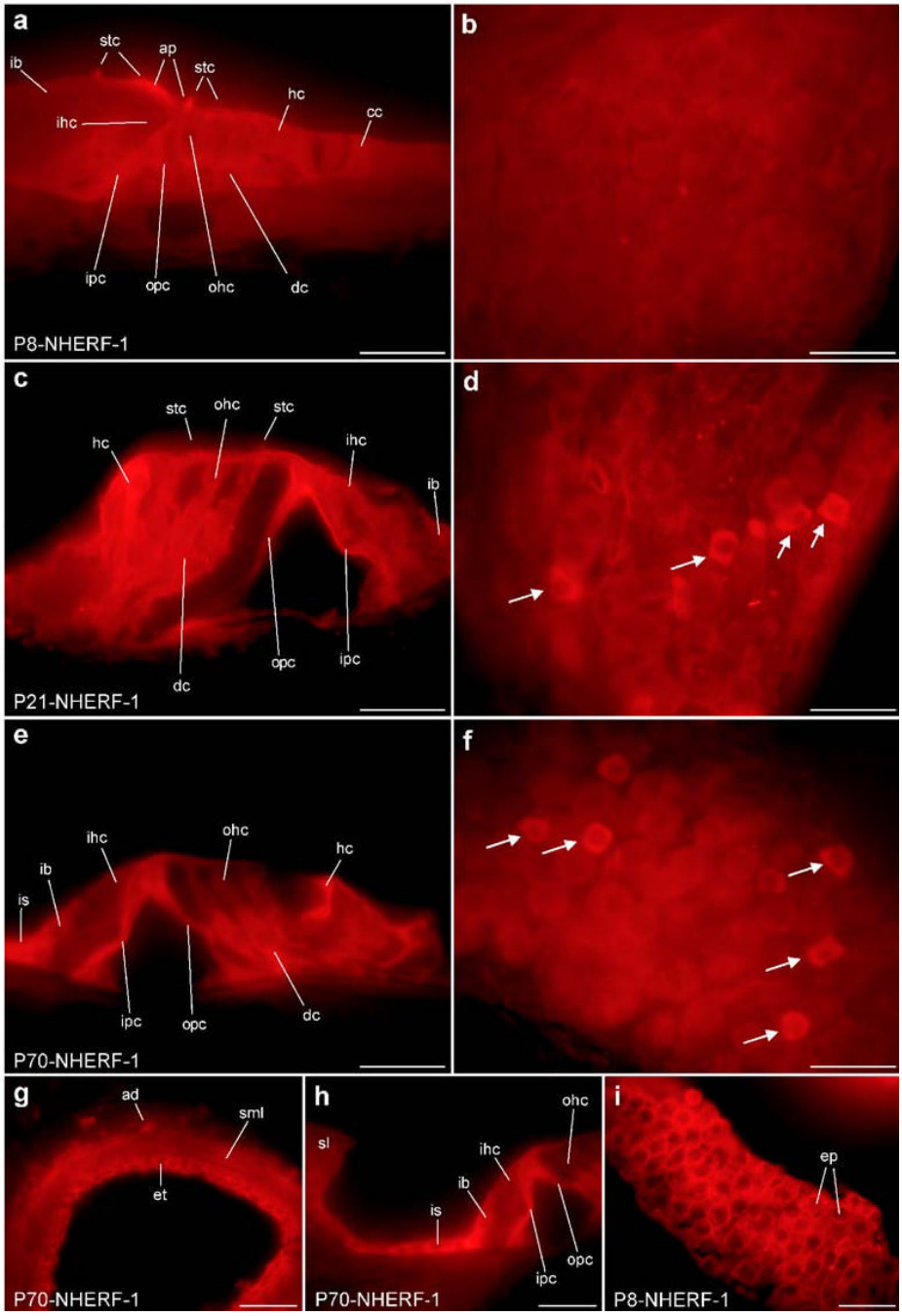

Fig. 3.

NHERF-1 immunolabeling in newborn (*P8*), juvenile (*P21*), and adult (*P70*) rat organ of Corti and spiral ganglion in cross section; conventional fluorescence microscopy. **a** In P8 organ of Corti, intense labeling was seen at the inner (IHC) and outer hair cell (OHC) stereocilia and apical end inner and outer pillar cells facing the endolymph. **b** In spiral ganglion neurons at P8, NHERF-1 labeling was low. **c** In organ of Corti at P21, the densest labeling was seen at Hensen's cells. Note the reduction in NHERF-1 labeling in comparison to P8 at hair cell stereocilia. **d** In spiral ganglion neurons at P21, NHERF-1 labeling was notably increased in a small subpopulation of neurons with small diameter cell bodies (*arrows*). **e** In organ of Corti at P70, NHERF-1 was very dense in Hensen's, inner and outer pillar, Deiters, and inner sulcus

cells. **f** In spiral ganglion at P70, NHERF-1 labeling was increased in most neurons, with higher levels being maintained in a subpopulation. **g** NHERF-1 labeling was observed in all layers of blood vessel walls, as seen here for a large artery (i.e., spiral modiolar artery) located in the modiolus adjacent to the cochlear nerve of a P70 rat. **h** NHERF-1 labeling was very dense in the inner sulcus cells of the adult organ of Corti. **i** Epithelial cells of the Reissner's membrane; a flat piece showing dense NHERF-1 labeling at P8. Abbreviations as in legend to Fig. 2. *Bar* 25 μm

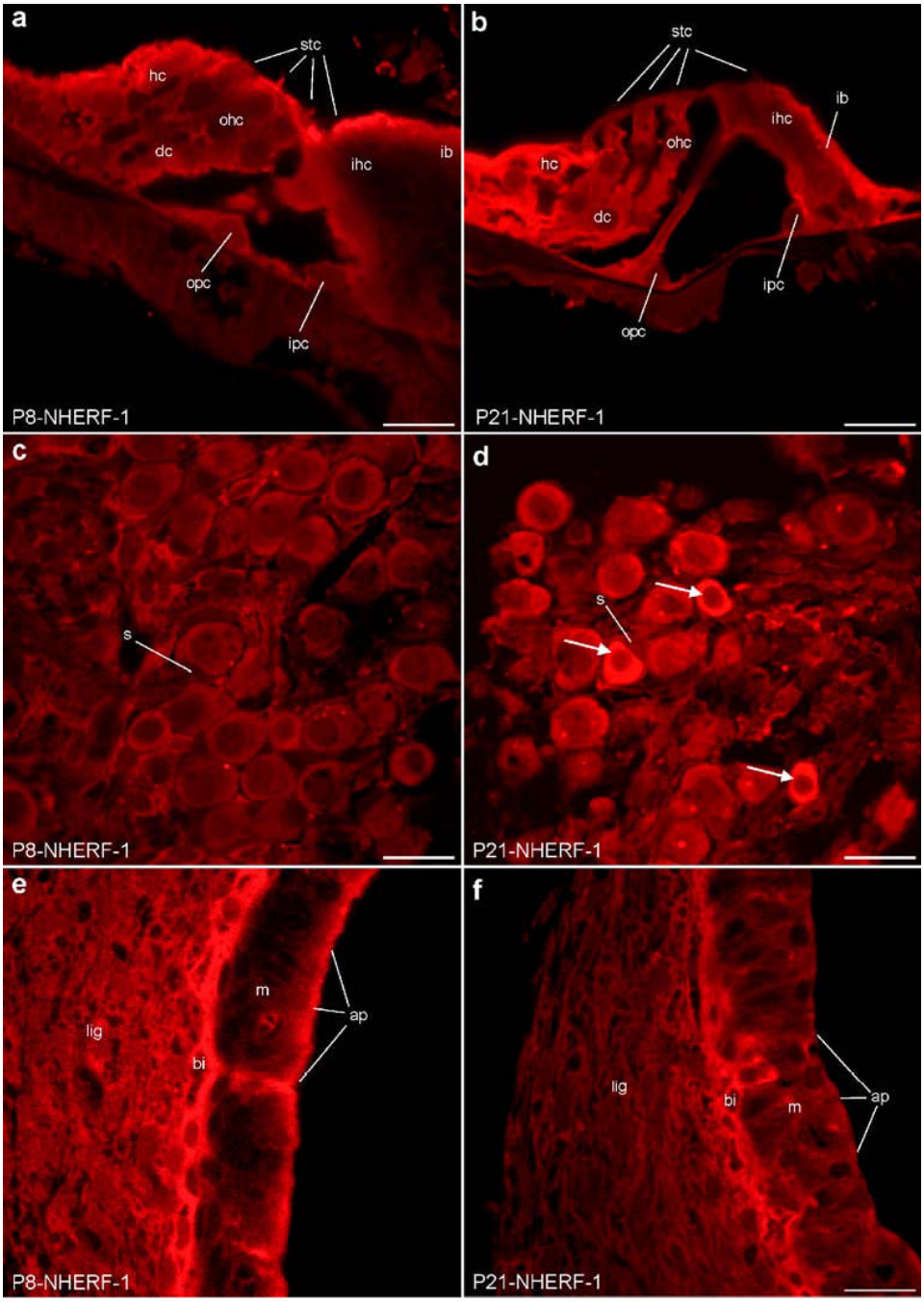

Fig. 4.

Confocal optical sections (1 μm) showing NHERF-1 labeling in the P8 and P21 organ of Corti, spiral ganglion, and stria vascularis in cross section. **a** Strong NHERF-1 labeling in the P8 organ of Corti was detected in the apical membranes of sensory hair cells and supporting cells lining the endolymphatic compartment, including developing hair cell stereocilia and cuticular plates at which the stereocilia are attached. **b** NHERF-1 labeling in P21 organ of Corti was significantly reduced in the apical membrane and stereocilia of hair cells but was increased in supporting cells including Hensen's, Deiters, pillar, and inner border cells. The labeling surrounding the outer hair cell (OHC) bodies belong to Deiters cell phalangeal (apical) processes extending toward the OHC cuticular plates. **c** NHERF-1 labeling in P8 spiral

ganglion neurons was weak and homogenous. Weak labeling was also evident in satellite cells attached to neurons. **d** At P21, neuronal NHERF-1 labeling intensity increased in the spiral ganglion, in particular in a small subpopulation of neurons with a smaller diameter. Labeling in the satellite cells remained unchanged. **e** NHERF-1 labeling in P8 stria vascularis was very strong in the basal and intermediate cell region and in the apical membrane of the marginal cells of the stria vascularis. **f** At P21, NHERF-1 labeling in the apical membrane of the marginal cells showed a marked reduction, whereas relatively dense labeling was maintained at the basal and intermediate cell region. Abbreviations as in legend to Fig. 2. *Bar* 25 μm

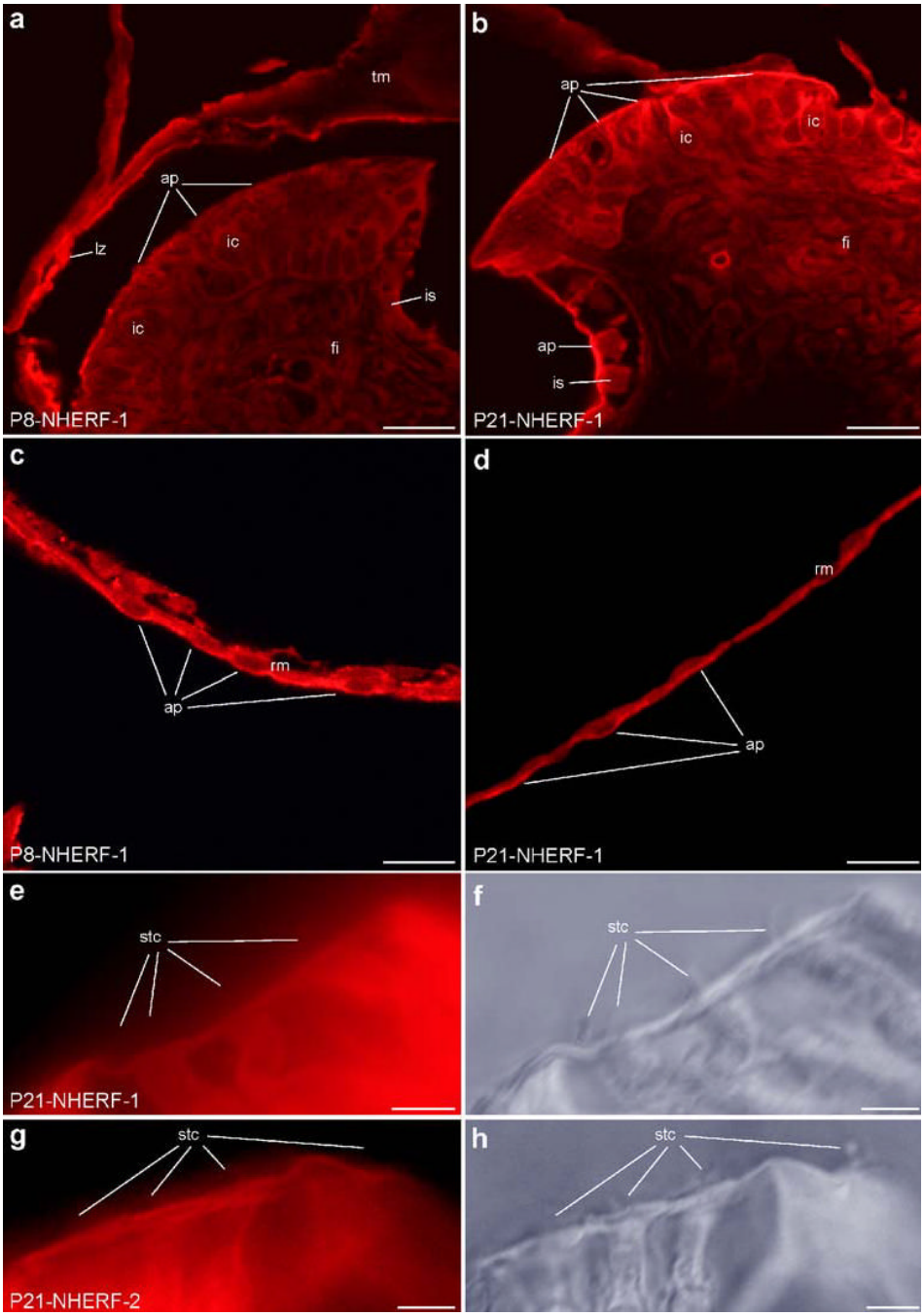

Fig. 5.

Confocal optical sections (1 μm) showing NHERF-1 labeling in the spiral limbus (*P8*, *P21*) and Reissners' membrane (*P8*). **a** NHERF-1 labeling at the P8 spiral limbus was weak in interdental cells and showed apical localization at the region of attachment of the tectorial and Reissners' membranes. Inner sulcus cells also showed weak labeling. Note the dense labeling at the limbal zone of the tectorial membrane. **b** At P21, NHERF-1 labeling in the interdental cells and inner sulcus cells showed a marked increase, particularly in their apical membranes. **c** NHERF-1 labeling in P8 Reissner's membrane was mostly confined to the apical membrane facing the endolymphatic compartment. **d** NHERF-1 labeling at the apical membrane of Reissner's epithelia was reduced after the onset of hearing. **e** Lack of labeling with NHERF-1

antibody of the P21 hair cell stereocilia, the structural integrity of which was confirmed by light microcopy (**f**). **g** Lack of NHERF-2 labeling of the P21 hair cell stereocilia, which were present as visualized by light microscopy (**h**). Abbreviations as in legend to Fig. 2. *Bars* 25 μm (**a**–**d**), 10 μm (**e**–**h**)

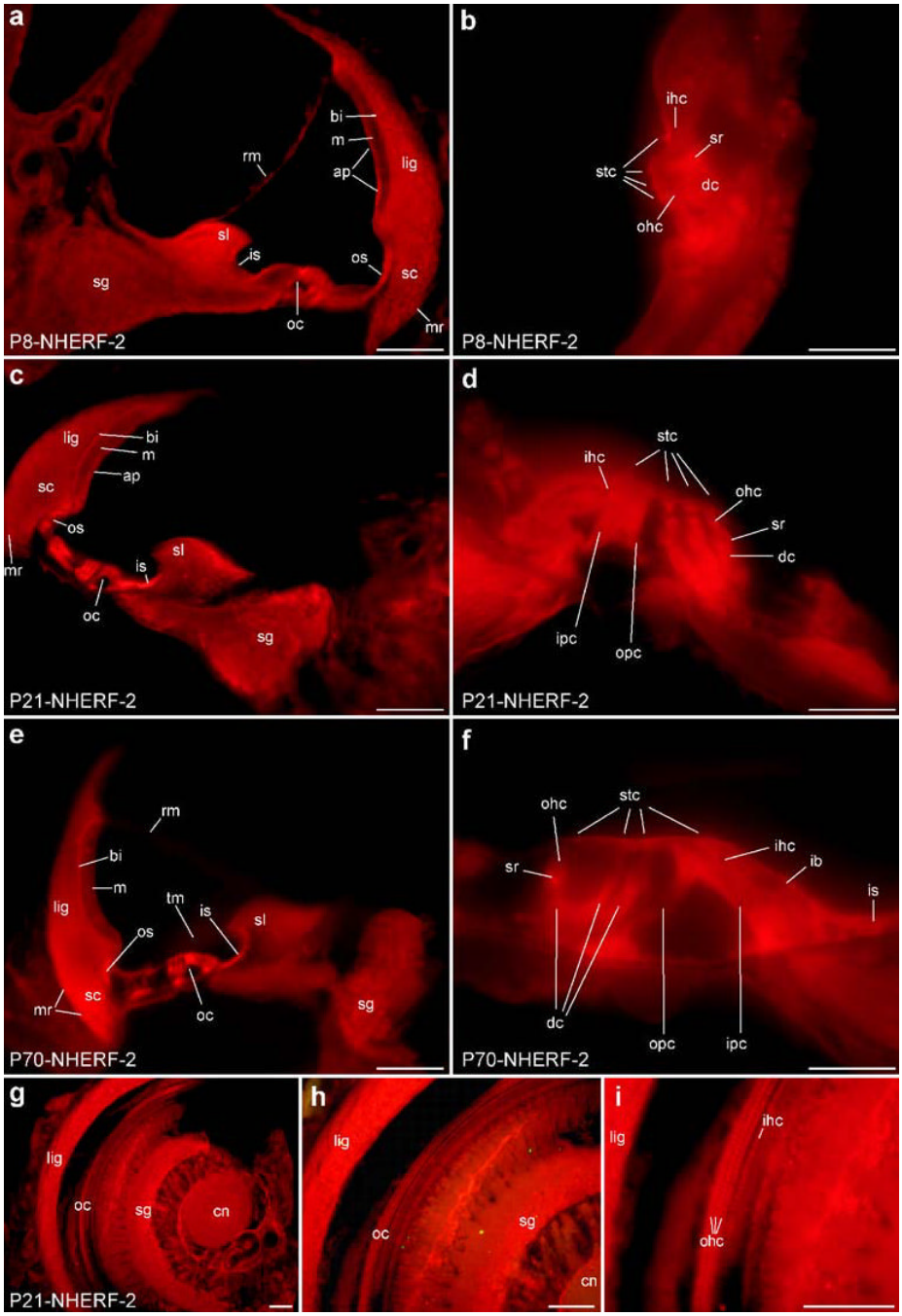

Fig. 6.

NHERF-2 immunolabeling in the newborn (*P8*), juvenile (*P21*), and adult (*P70*) rat cochlea in mid-modiolar (cross) and planar orientations; conventional fluorescence microscopy. **a**, **b** Wide-spread distribution of NHERF-2 labeling in P8 cochlea including stria vascularis, spiral limbus, Reissner's membrane (**a**) and organ of Corti (**b**) with dense labeling in the apical membrane and stereocilia of sensory and supporting cells. **c**, **d** Distribution of NHERF-2 labeling in P21 cochlea (**c**) and organ of Corti (**d**) showing increased levels of labeling in the spiral ganglion neurons and the synaptic region where they terminate underneath the OHC, supporting cells in the organ of Corti, and inner sulcus cells. At P21 organ of Corti, NHERF-2 labeling in the stereocilia and apical membranes of the cells lining endolymphatic compartment

is markedly reduced but is maintained at cuticular plates of hair cells. **e**, **f** Increased NHERF-2 labeling in the synaptic regions beneath the OHC and in supporting cells of the organ of Corti in which labeling in sensory hair cell bodies and stereocilia is absent, but maintained at cuticular plates, in P70 cochlea. **g**–**i** Wide-spread distribution of NHERF-2 labeling in planar plane of cochlea showing the spiral ligament, organ of Corti, and Rosenthal's canal including spiral ganglion neurons and cochlear nerve. Abbreviations as in legend to Fig. 2. *Bars* 100 μm (**a**, **c**, **e**, **g**–**i**), 25 μm (**b**, **d**, **f**)

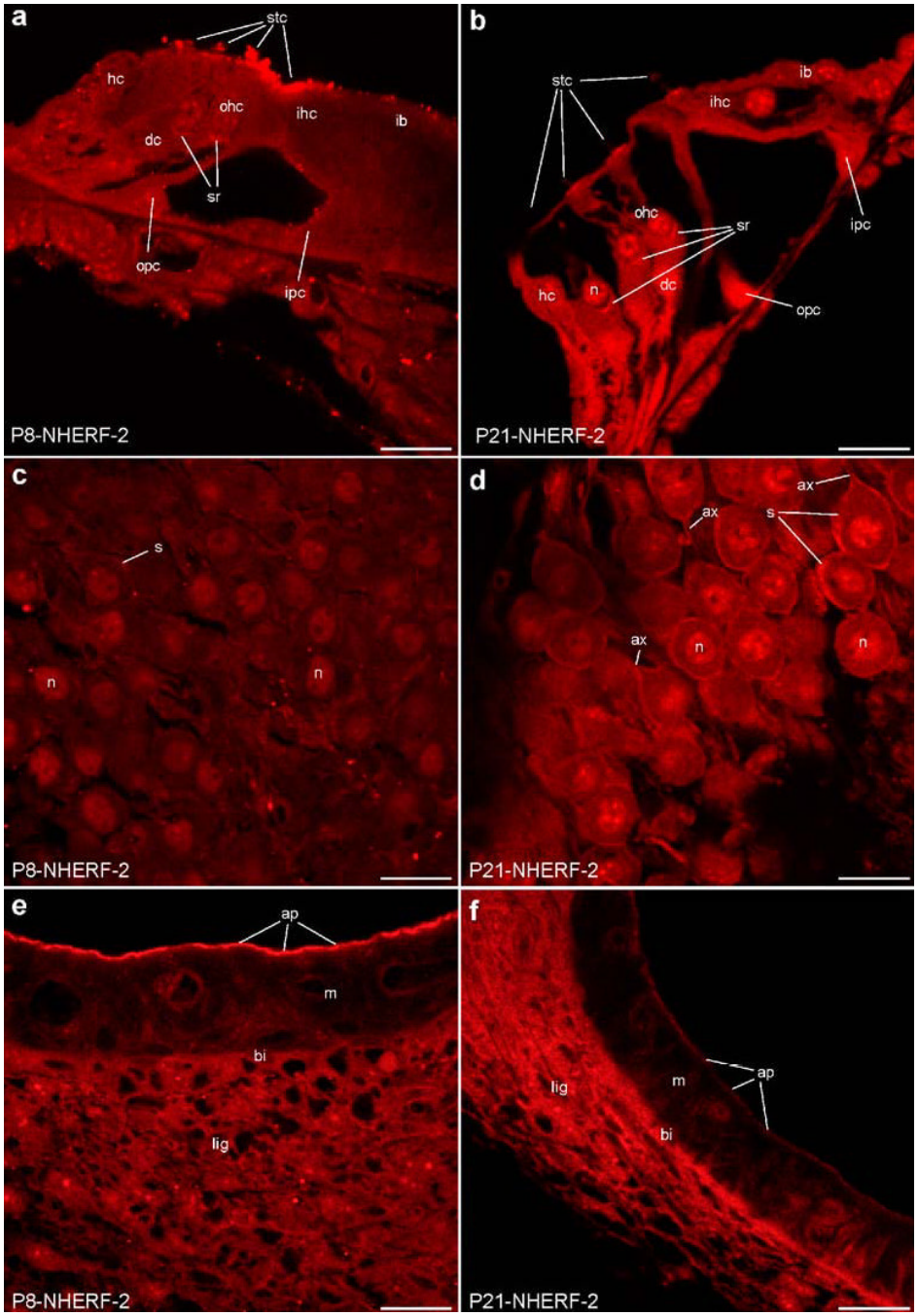

Fig. 7.

Confocal optical sections (1 μm) showing NHERF-2 labeling in the P8 and P21 organ of Corti, spiral ganglion, and stria vascularis in cross section. **a** In organ of Corti at P8, NHERF-2 labeling was dense at the apical surface including hair cell stereocilia. Weak labeling was also evident at the synaptic regions beneath the outer hair cells. **b** NHERF-2 labeling in the apical surface and hair cell stereocilia showed marked reduction in organ of Corti at P21, whereas labeling in OHC and IHC cuticular plates was maintained. NHERF-2 labeling was increased at the synaptic regions beneath the OHC and supporting cells including Hensen's, Deiters, inner border, and inner and outer pillar cells. Dense punctuate staining was associated with nucleus and/or nuclear membranes of hair cells and supporting cells. Dense NHERF-1 labeling

in the Hensen's, inner and outer pillar, Deiters, and inner sulcus cells. **c** Weak NHERF-2 labeling in spiral ganglion neurons of P8 cochlea was associated with punctuate labeling of nucleus and plasma membrane. Satellite cells also showed weak NHERF-2 labeling. **d** At P21, NHERF-2 labeling intensity in the spiral ganglion increased in neurons and satellite cells. Note that the NHERF-2 labeling is mostly associated with the plasma membrane, nucleus, and cellular processes (e.g., axonal membranes). **e** The P8 stria vascularis showed the densest NHERF-2 labeling in the apical membrane of marginal cells. Dense NHERF-2 labeling was also evident in the basal and intermediate cell layers and fibrocytes of the spiral ligament. **f** At P21, NHERF-2 labeling in the apical membrane of strial marginal cells was mostly reduced, whereas intensity increased at the basal and intermediate cell layers and spiral ligament fibrocytes. Abbreviations as in legend to Fig. 2. *Bars* 25 μm

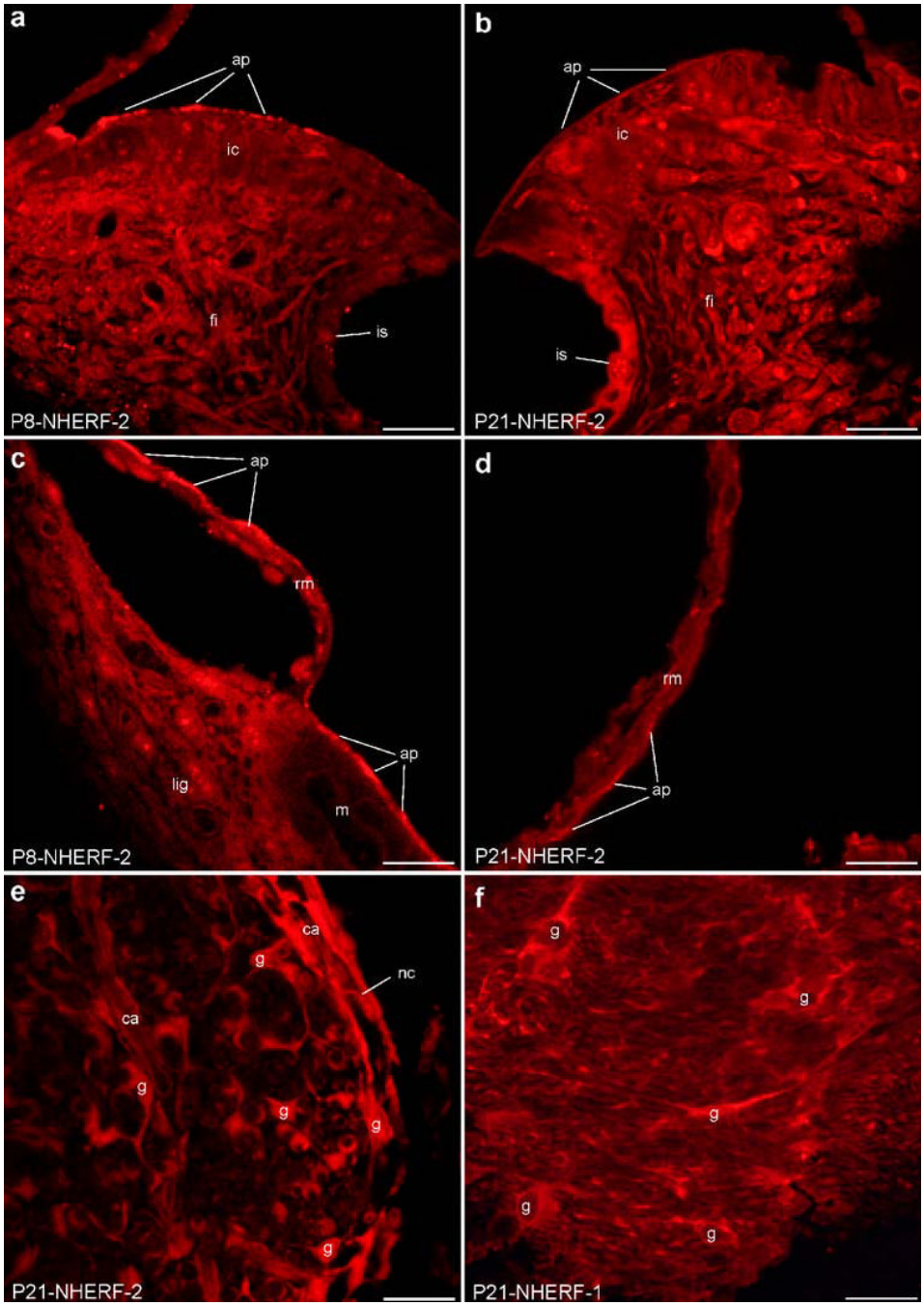

Fig. 8.

Confocal optical sections (1 μm) showing NHERF-2 labeling in the spiral limbus (*P8*, *P21*), Reissner's membrane (*P8*), and cochlear nerve glia (*P21*). **a** In the spiral limbus at P8, NHERF-2 labeling was intense at the apical membrane of interdental cells and the fibrocytes beneath. Inner sulcus cells showed weak labeling. **b** NHERF-2 labeling was reduced at the apical surface of interdental cells but increased at the inner sulcus cells. **c** At P8, dense NHERF-2 labeling in Reissner's membrane was mostly associated with the apical (endolymphatic) membrane of epithelial cells, as a continuation of the apical labeling in strial marginal cells. **d** Reduction in NHERF-2 labeling in the apical membrane of the Reissner's epithelia at P21. **e** Dense NHERF-2 labeling in the P21 cochlear nerve glial cell bodies and

processes associated with capillaries. Note that the labeling associated with nerve coverings is denser. **f** NHERF-1 labeling was moderate in glial cell bodies and their processes located in the cochlear nerve (P21). Abbreviations as in legend to Fig. 2. *Bars* 25 μm

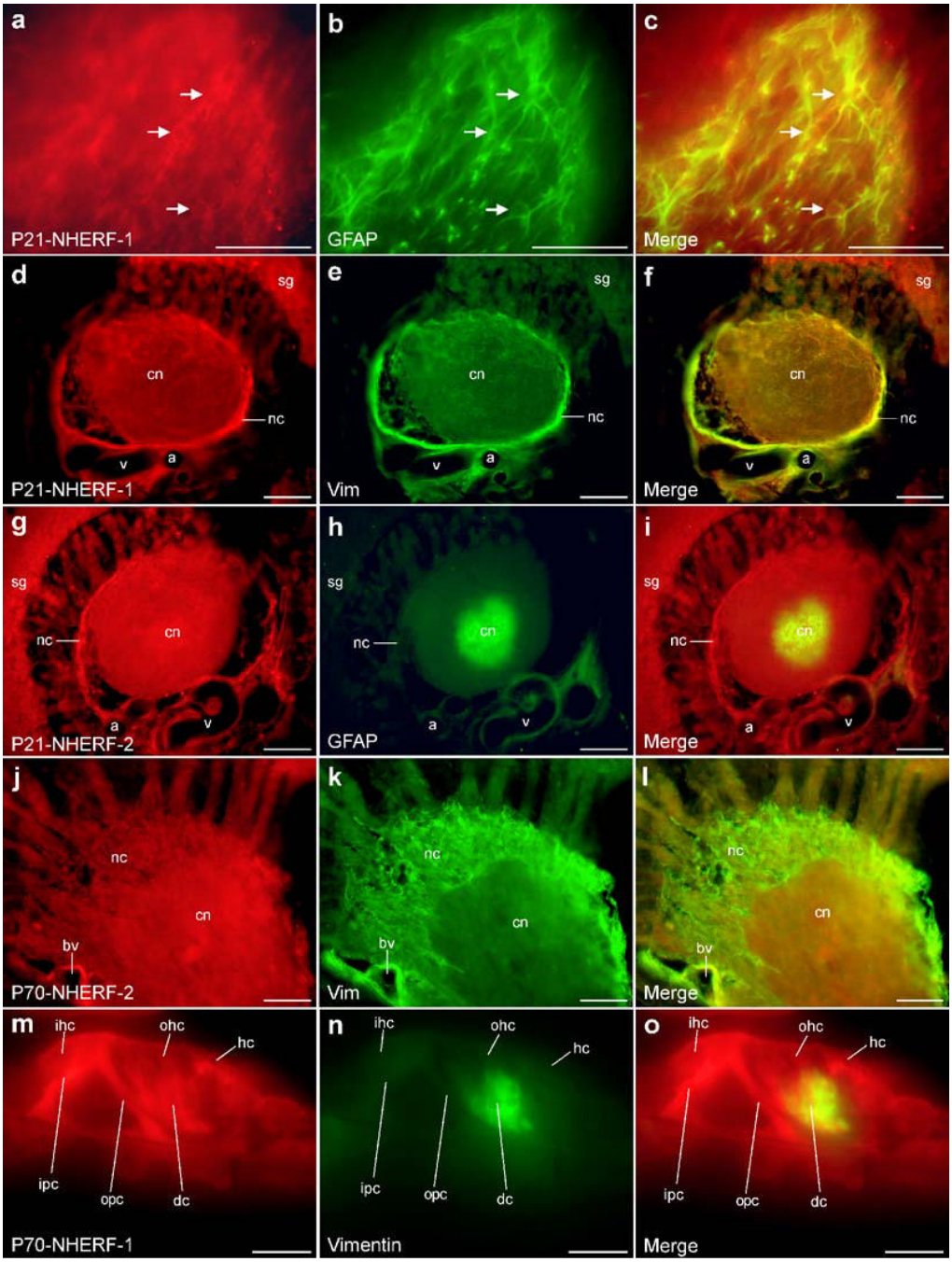

Fig. 9.

Co-localization of NHERF-1 and NHERF-2 with GFAP and vimentin. **a**–**c** NHERF-1 and GFAP are co-localized in glial cells of the cochlear nerve (*arrows*). **d**–**f** Co-localization of NHERF-1 and vimentin in cochlear nerve, nerve covering (epineurium), and large blood vessel (spiral modiolar artery and vein) walls and surrounding tissues. Large arteries and veins positioned next to each other were distinguished by the thickness of their walls and internal diameter, arteries having relatively thicker walls and smaller diameters. **g**–**i** Co-localization of NHERF-2 with GFAP-expressing glial cells in the cochlear nerve. **j**–**l** Co-localization of NHERF-2 and vimentin in the cochlear nerve, epineurium, and external layer of large blood vessels. **m**–**o** Co-localization of NHERF-1 and vimentin in Deiters cells of organ of Corti from

P70 rat. Note also the NHERF-1 labeling alone in the synaptic region beneath the OHC. Abbreviations as in legend to Fig. 2. *Bars* 100 μm (**a–l**), 25 μm (**m–o**)

Table 1

Relative and qualitative density levels of NHERF-1 and NHERF-2 immunolabeling in cochlear tissues at three postnatal stages

Region/cell type	Age	NHERF-1	NHERF-2
Inner and outer hair cells (stereocilia)	P8	++++	+++++
	P21	+	+
	P70	−	−
Inner and outer hair cells (cuticular plates)	P8	++++	++++
	P21	+++	+++
	P70	++	++
Synaptic regions beneath the outer hair cells	P8	−	++
	P21	+	+++
	P70	+	++++
Strial marginal cells (apical membranes)	P8	++++	++++
	P21	++	++
	P70	+	+
Basal and intermediate cell region of stria vascularis	P8	+++++	++
	P21	++++	+++
	P70	++++	+++
Reissner's membrane epithelia	P8	++++	+++
	P21	++	+
	P70	+	+
Inner sulcus cells	P8	+	+
	P21	++++	+++
	P70	+++++	+++
Outer sulcus cells	P8	++	++
	P21	++++	+++
	P70	++++	+++
Spiral limbus (interdental cells)	P8	++	++++
	P21	++++	++
	P70	++++	++
Hensen's cells	P8	++	++
	P21	+++++	+++
	P70	+++++	+++
Inner border cells	P8	++	++
	P21	+++	+++
	P70	+++++	+++
Deiters cells	P8	++	++
	P21	++++	++++
	P70	++++	++++
Inner and outer pillar cells	P8	++	++
	P21	++++	++++
	P70	+++++	++++
Spiral ganglion neurons	P8	++	++
	P21	++++	+++
	P70	++++	++++
Spiral ligament (fibrocytes)	P8	++	++
	P21	+++	+++
	P70	+++	+++
Claudius cells	P8	++	++
	P21	++	+
	P70	++	+
Limbal zone of tectorial membrane	P8	+++++	+++
	P21	+++	+
	P70	+	−
Tectorial membrane	P8	+++	++
	P21	++	+
	P70	−	−
Cochlear nerve (glia)	P8	++	+++
	P21	++	+++
	P70	++	+++
Walls of large blood vessels (artery and vein)	P8	+++	+++
	P21	++++	+++
	P70	++++	+++

The data were generated by conventional and confocal microscopic analysis of cochlear sections (minimum 50 sections per age group) by using 40× and 100× objectives. Immunolabeling density was scored as absent (−), threshold (+), moderate (++), dense (+++), very dense (++++), and saturating levels (+++++) for major cochlear structures